

Performance Enhancement of Photovoltaic Panels with a Silicon-Based Backsheet: An Experimental Study

Salaheldin Alous¹, Fawzi Elhamshri^{2*}, Muhammet Kayfeci³, Ali Uysal⁴

¹Department of Mechanical and Industrial Engineering, Faculty of Engineering, University of Zawia, Libya.

²Department of Chemical Engineering, Faculty of Engineering - Algaraboli, University of Elmergib, Libya.

³Department of Energy Systems, Faculty of Technology, Karabuk University, Turkey.

⁴Department of Mechatronics, Faculty of Technology, Manisa Celal Bayar University, Manisa, Turkey.

*Corresponding author email: faalhamashri@elmergib.edu.ly

Received: 16-10-2025 | Accepted: 02-12-2025 | Available online: 25-12-2025 | DOI:10.26629/jtr.2025.62

ABSTRACT

The electrical efficiency of the photovoltaic (PV) panels diminishes with rising cell temperatures, a key challenge in PV performance. While various passive cooling methods exist, there is a need for simple, integrated, and effective thermal management solutions. This study investigates the use of a silicon-based thermal isolator as a novel backsheets material to address this gap. A 0.25 mm Sil-Pad 400 sheet (Henkel) with a thermal conductivity of 0.9 W/m.K was laminated onto solar cells, replacing the standard Tedlar layer. The performance of the modified panel was evaluated against an identical reference panel through a single-day, side-by-side comparative test. This protocol, employing synchronized measurements of electrical output and surface temperature from 11:00 to 14:00, ensured that both panels were subjected to identical environmental conditions, thereby normalizing the effect of solar irradiance fluctuations. Results confirmed the superior thermal regulation of the silicon isolator panel, which exhibited average temperature reduction of 4 °C on the front surface, and 2 °C on the back surface, yielding a combined average reduction of 3 °C. This effective cooling translated directly into a significant 13% average increase in power output. These findings demonstrate that silicon-based isolators are a highly promising solution for enhancing PV efficiency and energy yield, offering a practical and scalable approach for improving the performance of real-world solar installations.

Keywords: Silicon Isolators, thermal conductivity enhancement, Performance, Photovoltaic panels (PV).

تحسين أداء الألواح الكهروضوئية باستخدام طبقة خلفية من السيليكون: دراسة

تجريبية

صلاح الدين العلوص¹, فوزي الهمشري², محمد كيفجي³, علي يوصل⁴

¹قسم الهندسة الميكانيكية والصناعية، كلية الهندسة ، جامعة الزاوية ، الزاوية، ليبيا.

²قسم الهندسة الكيميائية، كلية الهندسة - القره بوللي ، جامعة المربك، ليبيا.

³قسم أنظمة الطاقة، كلية التكنولوجيا، جامعة كاربوك، تركيا.

⁴قسم الميكاترونیات، كلية التكنولوجيا، جامعة مانسيا جلال بايار، مانسيا، تركيا.

ملخص البحث

تحفظ الكفاءة الحرارية للألواح الكهروضوئية (PV) مع ارتفاع درجة حرارة خلاياها، وهو تحدي رئيسي في أداء الألواح الكهروضوئية. مع وجود طرق تبريد سلبية متعددة، هناك حاجة إلى حلول بسيطة ومتكلمة وفعالة لإدارة الحرارة. تحقق هذه الدراسة في استخدام

عازل حراري سيلكوني كمواد خلفية جديدة لمعالجة هذه الفجوة. تم لصق لوح Sil-Pad 400 بسمك 0.25 مم (من شركة هيتك) بتوصيل حراري قدره $W/m.K$ 0.9 على الخلايا الشمسية ليحل محل طبقة التيدلار القياسية. تم تقييم أداء اللوح المعدل مع لوح مرجعي مطابق من خلال اختبار مقارن جنباً إلى جنب في يوم واحد. ضمن هذا البروتوكول، الذي استخدم قياسات متزامنة لمخرجات الكهربائية و درجة حرارة السطح من الساعة 11:00 الى الساعة 14:00، تعرض كلا اللوحين لظروف بيئية متطابقة، مما طبع أثر التغير في الإشعاع الشمسي. أكدت النتائج التفوق في التحكم الحراري للوح المعدل بالعازل السيلكوني، حيث أظهر متوسط انخفاض في درجة الحرارة قدره $^{\circ}C$ 4 على السطح الامامي، و $^{\circ}C$ 2 على السطح الخلفي، مما أسفر عن اجمالي انخفاض متوسط قدره $^{\circ}C$ 3. أدى هذا التبريد الى زيادة متوسطة في انتاج الطاقة قدره 13%. تظهر هذه النتائج أن العوازل القائمة على السيليكون هي حل واعد لتعزيز كفاءة الألواح الكهروضوئية و انتاج الطاقة، مما يقدم نهجا علميا قابلا للتطوير لتحسين أداء التطبيقات الشمسية في العالم الواقعي.

الكلمات الدالة: عوازل السيليكون، تعزيز التوصيل الحراري، الألواح الكهروضوئية.

1. Introduction

A highly promising solution to the challenges of rising energy demand and the green house effect -caused by the excessive use of fossil fuels- is the efficient harvesting and utilization of solar energy. Among the technologies that achieve this, photovoltaic (PV) panels are paramount. A PV panel is an assembly of solar cells, typically made from semiconductor materials, which are interconnected in series or parallel to form modules. These modules operate on the photovoltaic principle to convert directly into electrical power. Current analyses of future energy systems frequently overlook the essential role solar PV must play in meeting the 2030 and 2050 net-zero emissions milestones, despite its proven technological maturity[1]. Therefore, accelerating performance improvements through dedicated research and development is imperative. Solar cells primarily convert radiation from the visible portion of the solar spectrum into electrical energy. Radiation from the infrared and ultraviolet bands is largely not converted, instead generating heat that raises the cell's temperature. Consequently, the conversion efficiency of typical commercial photovoltaic panels, which depends on the solar cell technology and operating conditions, generally ranges from 13% to 20%[2]. The process of converting solar energy into electricity in photovoltaic cells can lead to

operating temperatures significantly above ambient, with elevations exceeding $50^{\circ}C$ [3]. Beyond including thermal stress, rising solar cell temperature reduces PV panel conversion efficiency at a rate of 0.4% to 0.65% per degree Celsius[4]. To mitigate the performance degradation caused by high operating temperatures in photovoltaic (PV) modules, active cooling is often employed[5]. This can be achieved using either fluid-based or solid based systems. Fluid cooling liquids or air, typically involves attaching heat exchanger to the rear of the PV panel and circulating a fluid to remove excess heat. Solid- based methods, on the other hand, often involve attaching materials with high thermal conductivity-such as aluminum or copper fins- to dissipate heat, or integrating phase change materials (PCMs) to absorb thermal energy[6]. A further method to limit temperature rise in PV modules is to improve their heat dissipation by enhancing the thermal conductivity of the rear layers. In the standard configuration, solar cells are encapsulated in sandwich structure comprising, from front to back: glass, ethylene-vinyl acetate (EVA), an anti-reflecting coating (ARC-Si), another EVA layer, and a Tedlar backsheets (a composite PET-PVF film from Dupont), as illustrated in Fig.1 . The thickness and material properties of each layer are detailed in Table 1[7]. In an experimental investigation, Stropnik and Stritić[8] utilized a phase change material

(PCM) to absorb heat from a PV panel and validated their findings against simulation results from TRANSYS software. They attached RT28HC PCM to the rear of a PV module and enclosed the assembly with acrylic glass, as shown in Fig.2. Their results demonstrated that the PV-PCM panel's surface temperature was 35.6 °C lower than that of a conventional panel over a daily cycle. Furthermore, simulation for a PV-PCM system in Ljubljana indicated a 7.3% increase in annual electricity production. In an experimental study, Lee et al.[7] enhanced the thermal conductivity of the rear EVA encapsulation layer by incorporating conductive fillers into the composite. With a filler content of 60 vol%, the thermal conductivities of composites filled with SiC, ZnO, and BN reached 2.85, 2.26, and 2.08 W/m.K respectively. The results confirmed that these modified EVA rear films significantly improve the cell's heat dissipation and overall PV efficiency. Pavgi et al. demonstrated the potential of thermally conductive backsheets (TCBs) to enhance both the performance and reliability of photovoltaic modules[9]. In a comparative field and laboratory study, modules with TCBs exhibited lower operating temperatures than those with conventional Tedlar-PET-Tedlar (TPT) backsheets, suggesting a path to increased energy yield. Furthermore, accelerated testing showed that selected TCBs maintained durability compared to standard modules, underscoring their viability as a reliable material for improving PV thermal management.

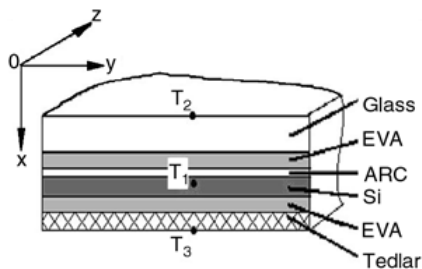


Fig1. Encapsulated Silicon solar cell Configuration[10].

This study aims to investigate the use of silicon isolator sheet as an economical, effective, and

simple thermal management solution for photovoltaic (PV) panels. Silicon isolators, a class of silicone rubber materials, are known for their excellent electrical insulation and superior heat transfer properties, making them common as thermal interface materials and heat sinks on electronic applications. They are commercially available in various forms such as sheets, gels, and adhesives. In this work, a sheet-type silicon isolator is attached to the rear of a PV panel to experimentally evaluate its impact on cell temperature and overall electrical performance.

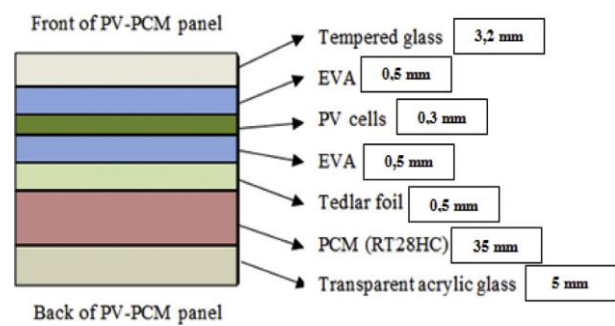


Fig 2. Schematic diagram of the PV-PCM panel after modification[8].

2. Methodology

For the experimental setup, a PV panel was fabricated in which a silicon isolator sheet replaced the standard Tedlar backsheets. The panel was laminated using a six layer structure, arranged as follows from top to bottom: tempered glass, ethylene-vinyl acetate (EVA), solar cells strings, EVA, the silicon isolator, and an aluminium sheet. This assembly was placed in a lamination machine and heated to 135 °C for approximately 22 minutes. After cooling, the excess EVA and isolator material were trimmed, a junction box was attached, and the laminate was framed. Fig. 3 presents a schematic diagram of the layer arrangement and the thickness of each layer in the final construction. Figure 4 shows the final manufactured silicon isolator PV panel. The electrical properties of both the silicon isolator and PV panels are listed in Table 2.

The experimental setup, shown in Fig. 5, consists of two PV modules mounted side-by-

side: the modified panel with a silicon isolator and a standard panel for reference. The silicon isolator used was a Sil-Pad 400 sheet supplied by Henkel Electronics Materials, with its properties detailed in Table 3. Temperature data were acquired using two thermocouples per panel (attached to the top and bottom surfaces) and an ambient temperature sensor, all connected to Picolog TC-8 data logger. Simultaneously, the current and voltage output of each panel were measured directly using separate MASTECH MY-68 multimeters.



Fig 3. Schematic diagram for silicon isolator PV panel.

To assure the reliability of the measurements and study results, it is important to estimate firstly the uncertainty in the measured parameters. A statistical approach can be used to estimate the uncertainty (w) in (N) measurements of a certain parameter (x) as follows [11]

$$x_m = \frac{1}{N} \sum x_i \quad (1)$$

$$S = \sqrt{\frac{1}{(N-1)} \sum (x_i^2 - x_m^2)} \quad (2)$$

$$a = \frac{1}{\sqrt{N}} \quad (3)$$

$$w = \sqrt{\sum_{i=1}^r a_i^2 \cdot S_i^2} \quad (4)$$

where (S) is the standard deviation. Table 4 represents the maximum experimental uncertainties w of the measured parameters related to the transducers used in the experimental and calculated by the Eq. (4). The maximum uncertainties in the calculated electrical power can be determined as following: The uncertainty (w_R) in a function

(R) of independent linear parameters (x_1, x_2, \dots, x_n) is given as [12]:

$$w_R = \left[\left(\frac{\partial R}{\partial x_1} w_1 \right)^2 + \left(\frac{\partial R}{\partial x_2} w_2 \right)^2 + \dots + \left(\frac{\partial R}{\partial x_n} w_n \right)^2 \right]^{1/2} \quad (5)$$

where: (w_1, w_2, \dots, w_n) the uncertainties in the independent parameters (x_1, x_2, \dots, x_n). Assume that parameters ($x_1, x_2, \dots, x_m, x_{m+1}, \dots, x_n$) are measured with uncertainties ($w_1, w_2, \dots, w_m, w_{m+1}, \dots, w_n$), and the function (R) is:

$$R = \frac{x_1 \times x_2 \times \dots \times x_m}{x_{m+1} \times x_{m+2} \times \dots \times x_n} \quad (6)$$

If the uncertainty in ($x_1, x_2, \dots, x_m, x_{m+1}, \dots, x_n$) are independent, then the fractional uncertainty in the function (R) is expressed as [13]:

$$\frac{w_R}{R} = \left[\left(\frac{w_1}{x_1} \right)^2 + \left(\frac{w_2}{x_2} \right)^2 + \dots + \left(\frac{w_m}{x_m} \right)^2 + \left(\frac{w_{m+1}}{x_{m+1}} \right)^2 + \dots + \left(\frac{w_n}{x_n} \right)^2 \right]^{1/2} \quad (7)$$

Appling the maximum uncertainties, which listed in Table 4, over the measurements range in Eq. (7), the maximum uncertainty in calculated electrical power is 2%

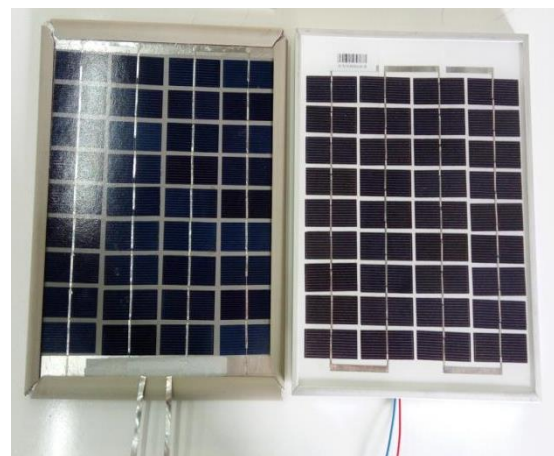


Fig 4. Silicon isolator PV panel (left) and standard PV panel (right).

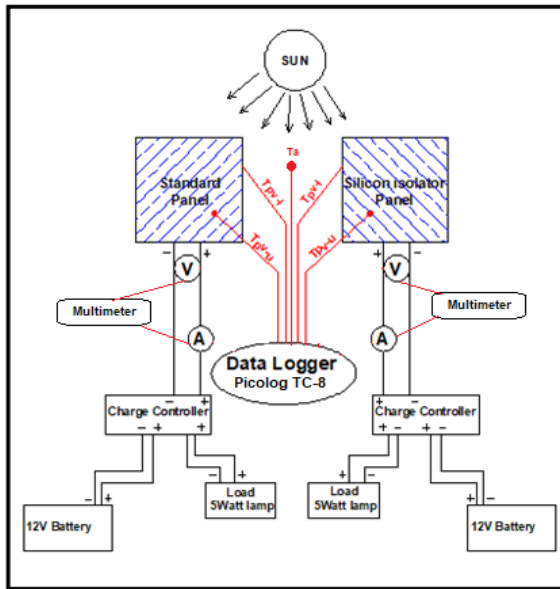


Fig5. Schematic diagram of the experimental setup.

3. RESULTS AND DISCUSSION

Due to the absence of irradiance data, this study focused on a direct, side by side comparison of the silicone isolator panel against the reference panel under identical conditions. For this specific goal, the single-day testing protocol was designed to ensure validity within its defined scope. To mitigate the lack of irradiance data and ensure a meaningful comparison, the experiment was conducted in two phases:

Phase1: Performance Comparison: Both panels were tested simultaneously on a day from 11:00 to 1400. During this period, seven synchronized measurement sets were taken for both panels. By measuring electrical power (current and Voltage), front surface temperature, and back surface temperature, in addition to ambient air temperature. All these measurements represented in figures 6, 7, and 8. The synchronized electrical measurements mean that any fluctuation in solar radiation affected both panels equally, allowing the difference in their power output to be attributed to their intrinsic performance. Crucially, the synchronized temperature measurements provide direct insight into the primary

mechanism behind any performance difference. Since PV cell efficiency is strongly dependent on operating temperature, the correlation between lower temperature readings and higher power output in the test panel serves as a key performance indicator, effectively compensating for the lack of irradiance data by explaining the electrical results.

Phase2: Thermal Performance Analysis: The continuous temperature logging was conducted over 40-mnutes period, under the same conditions. This ensures that panels were subjected to an identical solar radiation, allowing for a clear and fair comparison of their thermal properties.

Figures 6 and 7 present the front and back surface temperatures, respectively, for both the standard and silicon isolator panels, alongside the ambient temperature. Figure 8 shows the corresponding electrical power generated by both panels, calculated from synchronized current and voltage measurements. Collectively, Figures 6,7, and 8 present the results from phase1 (Performance Comparison).

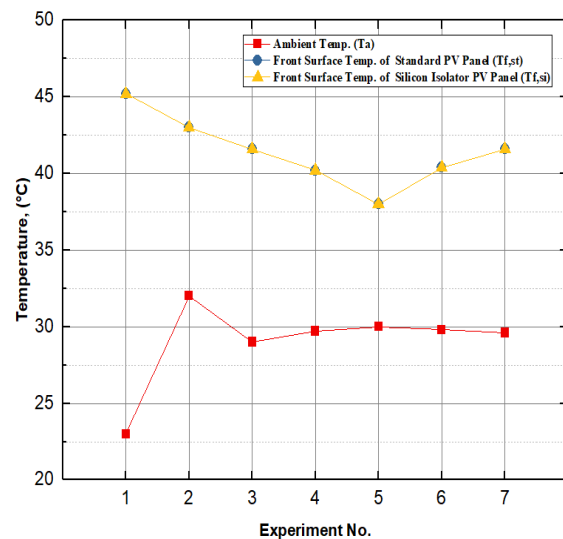


Fig 6. Measured temperatures of the front surface for Both standard and silicone isolator panels.

Comparative analysis confirmed a significant power generation advantage for the silicon isolator panel over the standard panel. The percentage increase in power output varied,

reaching a maximum of 19.78% (0.407 W) and a minimum of 1.93% (0.05 W). This percentage was calculated using the following formula:

$$\% \text{ increase} = \frac{P_{Si} - P_{ST}}{P_{ST}} \times 100$$

Where P_{Si} is the power of silicon isolator panel and P_{ST} is the power of the standard panel. The trend of this percentage increase is depicted in Fig. 9, which shows that the silicon isolator panel generated an average of 13% more electrical power than the standard panel.

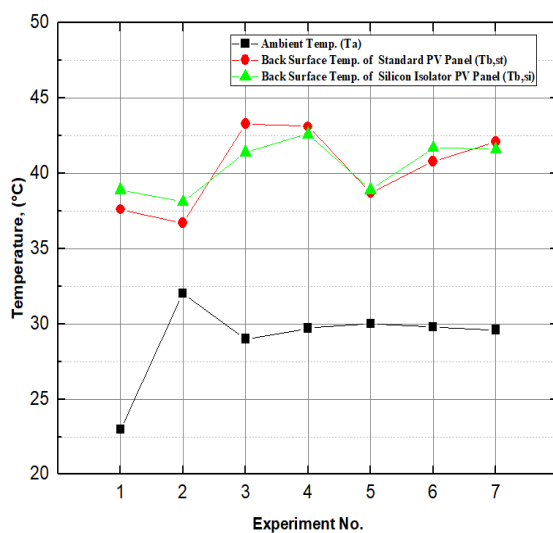


Fig 7. Measured temperatures of the back surface for Both standard and silicone isolator panels.

In the second phase (thermal Performance Analysis), which is performed in the yard of Energy Systems Laboratory, Karabuk University, the front and back surface temperatures of both the silicon isolator and standard panels were recorded continuously. Data was recorded at rate of 10 samples per second over a 41-second period to investigate the thermal regulation effect of the silicon isolator. The resulting temperature profiles are presented in figures 10 and 11. These figures clearly show that use of the silicon isolator reduced the temperature of both the front and back surfaces of the modified panel compared to the standard panel.

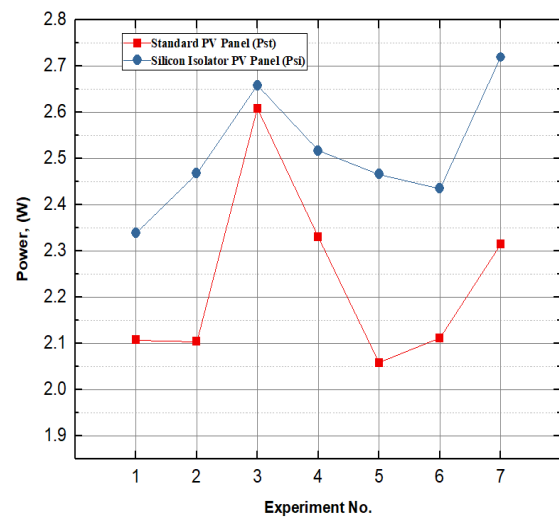


Fig 8. Power generation in standard and silicon isolator panels.

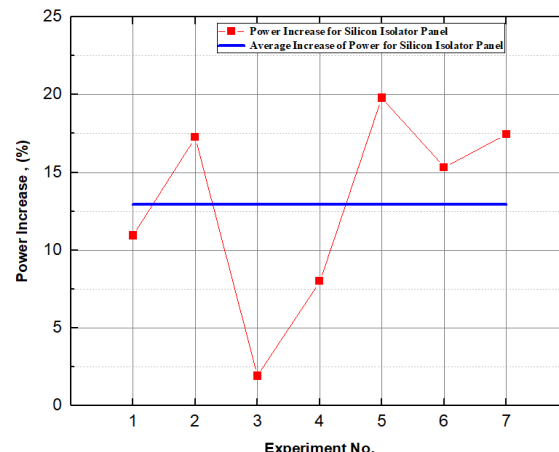


Fig 9. Percentage of power increase for silicon isolator.

The decline in temperature profiles observed in figures 10 and 11 was caused by a reduction in solar irradiance from cloud cover, a condition to which both panels responded simultaneously.

As shown in figure 10 and 11, the silicon isolator panel exhibited an average temperature reduction of 4 °C on the front surface and 2 °C on the back surface compared to the standard panel.

The profile of the temperature difference between the averaged cell temperatures of the two panels is presented in figure 12, revealing an overall average difference of 3 °C on favor of the silicon isolator panel

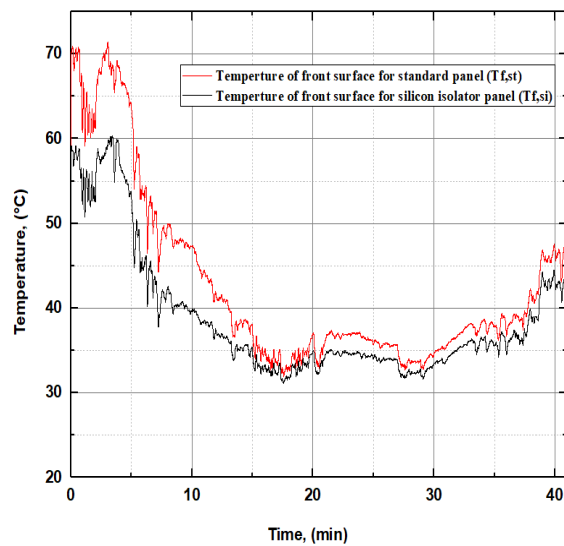


Fig 10. Measured temperatures of the front surface for Both standard and silicone isolator panels.

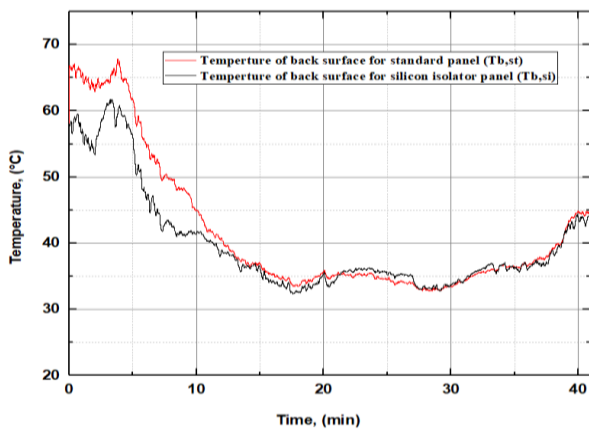


Fig 11. Measured temperatures of the back surface for Both standard and silicone isolator panels.

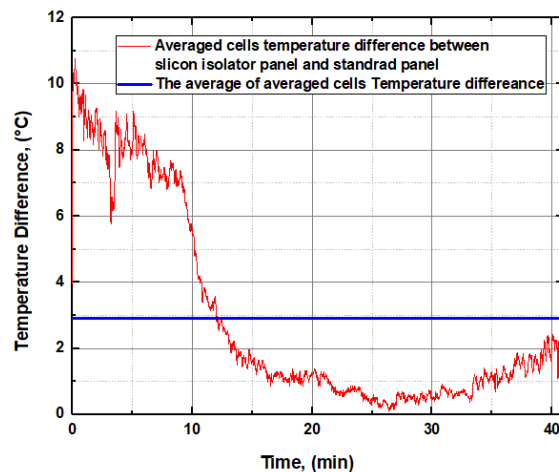


Fig 12. Average cells temperature difference between silicon isolator and standard panel.

The results clearly demonstrate that replacing the tedlar layer with a silicone isolator enhanced heat dissipation, leading to lower solar cell temperatures in the modified panel compared to the standard panel.

4. CONCLUSIONS

This study experimentally investigated the use of a 0.25 mm silicon isolator sheet (0.9 W/m.K) as a replacement for the standard Tedlar backsheets in a photovoltaic (PV) panel. The modified panel was fabricated by laminating the silicon isolator onto the solar cells at 135 °C for 22 minutes. Its performance was evaluated through a side-by-side outdoor comparison with a conventional panel of identical specifications

The results demonstrate that the silicon isolator significantly enhanced thermal management. The modified panel exhibited average temperature reductions of 4 °C on the front surface and 2 °C on the back surface compared to the standard panel. This improved heat dissipation directly translated to a substantial increase in electrical power output, with an overall average power gain of 13%. The instantaneous power enhancement ranged from 1.93% (0.05W) to a maximum of 19.78% (0.407 W).

These findings have direct practical implications for improving PV performance, particularly in hot climates where efficiency losses from elevated temperatures are most severe. The silicon isolator presents a simple, passive, and potentially cost-effective solution to mitigate these losses. Potential applications include its integration into new PV module manufacturing as a superior backsheets material, as well as its use in retrofitting existing installations to enhance their energy yield and operational lifespan. By maintaining lower operating temperatures, this approach can significantly boost the daily energy output and improve the long-term economic returns of solar power systems in sun-rich, high-temperature regions.

Based on these promising results, it is recommended that future work explores the integration of silicon isolators into full-scale PV modules and conducts long-term reliability studies to assess their durability and performance over various seasonal conditions.

5. ACKNOWLEDGMENT

Table 1. Sizes and properties of each layer in encapsulated Si solar cells.

No.	Layer	Thickness (δ) (mm)	Thermal conductivity (k) (W/m.k)
1	Glass	3.0	0.98*
2	EVA	0.5	0.23*
3	ARC	(0.06-0.1).10-3	1.38
4	Si	0.25-0.4	148
5	EVA	0.5	0.23*
6	Tedlar	0.1	0.36*

Table 2. properties. OF Silicon isolator and standard panel.

Property.	Value	
	Silicon isolator panel	Standard 5Watt Polycrystalline
Maximum Power (Pmax)	17 W	16,9 W
Maximum Power Current (Imp)	0.28 A	0.28 A
Open circuit voltage (Voc)	22.0 V	22.0 V
Short circuit current (Isc)	0.30 A	0.30 A
Cell type	Polycrystalline	Polycrystalline
Dimension	240 x 240x 8 (mm)	240 x 240 x10 (mm)

Table 3. Silicon isolator and standard panel properties.

TYPICAL PROPERTIES OF SIL-PAD 400					
PROPERTY	IMPERIAL VALUE	METRIC VALUE	TEST METHOD		
Color	Gray	Gray	Visual		
Reinforcement Carrier	Fiberglass	Fiberglass	—		
Thickness (inch) / (mm)	0.007, 0.009	0.178, 0.229	ASTM D374		
Hardness (Shore A)	85	85	ASTM D2240		
Breaking Strength (lbs/inch) / (kN/m)	30	5	ASTM D1458		
Elongation (% at 45° to Warp and Fill)	54	54	ASTM D412		
Tensile Strength (psi) / (MPa)	3000	20	ASTM D412		
Continuous Use Temp (°F) / (°C)	-76 to 356	-60 to 180	—		
ELECTRICAL					
Dielectric Breakdown Voltage (Vac)	3500, 4500	3500, 4500	ASTM D149		
Dielectric Constant (1000 Hz)	5.5	5.5	ASTM D150		
Volume Resistivity (Ohm-meter)	10^{11}	10^{11}	ASTM D257		
Flame Rating	V-O	V-O	UL 94		
THERMAL					
Thermal Conductivity (W/m-K)	0.9	0.9	ASTM D5470		
THERMAL PERFORMANCE vs PRESSURE					
Pressure (psi)	10	25	50	100	200
TO-220 Thermal Performance (°C/W) 0.007"	6.62	5.93	5.14	4.38	3.61
TO-220 Thermal Performance (°C/W) 0.009"	8.51	7.62	6.61	5.63	4.64
Thermal Impedance (°C-in ² /W) 0.007" (1)	1.82	1.42	1.13	0.82	0.54
Thermal Impedance (°C-in ² /W) 0.009" (1)	2.34	1.83	1.45	1.05	0.69

I) The ASTM D5470 test fixture was used. The recorded value includes interfacial thermal resistance. These values are provided for reference only. Actual application performance is directly related to the surface roughness, flatness and pressure applied.

Table 4. Maximum experimental uncertainties of the measured parameters.

Transduser	Measured Parameter	Maximum experimental uncertainty
K-type thermocouple connected to Piolog TC-8 data logger.	Amient, PV panel, and PVT collector front and back surface temperatures.	± 0.8 °C
Multimeter	Voltage.	± 0.05 V
	Current	± 0.004 A

REFERENCES

[1] Victoria M, et al. Solar photovoltaics is ready to power a sustainable future. Joule. 2021;5(5):1041–56.

[2] Armstrong S, Hurley WG. A thermal model for photovoltaic panels under varying atmospheric conditions. Appl Therm Eng. 2010;30(11):1488–95.

[3] Chow TT. A review on photovoltaic/thermal hybrid solar technology. Appl Energy. 2010;87(2):365–79.

[4] Ma T, Yang H, Zhang Y, Lu L, Wang X. Using phase change materials in photovoltaic systems for thermal regulation and electrical efficiency improvement: A review and outlook. Renew Sustain Energy Rev. 2015;43:1273–84.

[5] Makki A, Omer S, Sabir H. Advancements in hybrid photovoltaic systems for enhanced solar cells performance. Renew Sustain Energy Rev. 2015;41:658–84.

[6] Hamzat AK, Sahin AZ, Omisanya MI, Alhems LM. Advances in PV and PVT cooling technologies: A review. Sustain Energy Technol Assess. 2021;47:101360.

[7] Lee B, Liu JZ, Sun B, Shen CY, Dai GC. Thermally conductive and electrically insulating EVA composite encapsulants for solar photovoltaic (PV) cell. eXPRESS Polym Lett. 2008;2(5):357–63.

[8] Stropnik R, Stritih U. Increasing the efficiency of PV panel with the use of PCM. Renew Energy. 2016;97:671–9.

[9] Pavgi A, Oh J, Tatapudi S, TamizhMani G. Performance and reliability of thermally conductive backsheets (TCB). In: 2020 47th IEEE Photovoltaic Specialists Conference (PVSC). 2020. p. 775–80.

[10] Lu ZH, Yao Q. Energy analysis of silicon solar cell modules based on an optical model for arbitrary layers. Sol Energy. 2007;81(5):636–47.

[11] Ceylan İ, Ergun A. Thermodynamic analysis of a new design of temperature controlled parabolic trough collector. Energy Convers Manag. 2013;74:505–10.

[12] Kline SJ. Describing uncertainty in single sample experiments. Mech Eng. 1953;75:3–8.

[13] Taylor J. Introduction to error analysis: The study of uncertainties in physical measurements. 1997.